

Comparative Evaluation of Generative AI Models for Chest Radiograph Report Generation in the Emergency Department

Original Research

Woo Hyeon Lim, MD,^{a,*} Ji Young Lee, MD, PhD,^{a,*} Jong Hyuk Lee, MD, PhD,^{a,b} Saehoon Kim,
PhD,^{c,†} Hyungjin Kim, MD, PhD^{a,b,c,†}

^aDepartment of Radiology, Seoul National University Hospital, 101 Daehak-ro, Jongno-gu, Seoul 03080, Korea; ^bDepartment of Radiology, Seoul National University College of Medicine, 101 Daehak-ro, Jongno-gu, Seoul 03080, Korea; ^cSoombit.ai, 21 Pangyo-ro 255-gil, Bundang-gu, Seongnam 13486, Korea

*These authors contributed equally to this study as co-first authors.

†These authors contributed equally to this study as co-senior authors.

Address correspondence to:

Hyungjin Kim, MD, PhD. Department of Radiology, Seoul National University College of Medicine, 101 Daehak-ro, Jongno-gu, Seoul, 03080, Korea. Tel: 82-2-2072-2254, Fax: 82-2-743-6385, E-mail: khj.snuh@gmail.com

Abstract

Background: Medical domain vision–language models (VLMs) have recently been introduced for chest radiograph (CXR) report generation. Comparative evaluation is essential to assess their clinical applicability.

Purpose: To benchmark open-source or commercial medical image–specific VLMs against real-world radiologist-written reports, focusing on diagnostic quality, clinical acceptability, hallucinations, and language clarity.

Methods: This retrospective study included adult patients who presented to the emergency department of a tertiary center between January 2022 and April 2025 and underwent same-day CXR and CT for febrile or respiratory symptoms. Reports from five VLMs (AIRead, Lingshu, MAIRA-2, MedGemma, and MedVersa) and radiologist-written reports were randomly presented and blindly evaluated by three thoracic radiologists using four criteria: RADPEER, clinical acceptability, hallucination, and language clarity. Comparative performance was assessed using generalized linear mixed models, with radiologist-written reports treated as the reference. Finding-level analyses were also performed with CT as the reference.

Results: A total of 478 patients (median age, 67 years [interquartile range, 50–78]; 282 men [59.0%]) were included. AIRead demonstrated the lowest RADPEER 3b rate (5.3% [76/1434] vs. radiologists 13.9% [200/1434]; $P<.001$), whereas other VLMs showed higher disagreement rates (16.8–43.0%; $P<.05$). Clinical acceptability was the highest with AIRead (84.5% [1212/1434] vs. radiologists 74.3% [1065/1434]; $P<.001$), while other VLMs performed worse (41.1–71.4%; $P<.05$). Hallucinations were rare with AIRead, comparable to radiologists (0.3% [4/1425]) vs. 0.1% [1/1425]; $P=.21$), but frequent with other models (5.4–17.4%; $P<.05$). Language clarity was higher with AIRead (82.9% [1189/1434]), Lingshu (88.0% [1262/1434]), and MedVersa (88.4% [1268/1434]) compared with radiologists (78.1% [1120/1434]; $P<.05$). Finding-level analyses showed substantial variability in sensitivity across VLMs for the common findings (i.e., lung opacity, pleural effusion, cardiomegaly, and emphysema): AIRead,

15.5–86.7%; Lingshu, 2.4–86.7%; MAIRA-2, 6.0–72.0%; MedGemma, 4.8–76.7%; and MedVersa, 20.2–69.3%.

Conclusion: Medical VLMs for CXR report generation exhibited variable performance in report quality and diagnostic measures.

Introduction

Over the past decade, artificial intelligence (AI)-based approaches, including deep learning, have shown promise in detecting and localizing abnormalities in chest radiographs (CXRs)¹. More recently, the emergence of vision–language models (VLMs), which jointly process images and text, has brought attention to radiologic report generation¹. This is particularly relevant in light of the global shortage of radiologists, which is increasingly strained by the growing demand and clinical importance of imaging studies^{2,3,4}. VLM-based report generation has therefore been proposed as a potential solution for producing timely and clinically useful reports in settings with limited radiologist availability¹.

Previous studies have explored the performance of AI in CXR report generation, most often evaluating outputs with semantic similarity measures or automated metrics based on label extraction^{5,6,7,8}. However, assessing the clinical utility and quality of AI-generated reports requires a multifaceted approach to accurately determine the readiness of VLMs for clinical translation^{9,10}. For instance, one prior study employed multidimensional assessments including clinical acceptability, expert agreement, and overall report quality¹⁰. Key dimensions of VLM-generated report evaluation should encompass diagnostic performance (report-level and finding-level), clinical acceptability (i.e., whether generated reports are suitable for clinical use with only minor revisions), absence of hallucination, and linguistic clarity^{10,11}.

Medical image–specific VLMs can internalize radiology priors beyond what generalist models acquire from natural images and captions^{10,11,12}. Although medical VLMs have demonstrated promising performance in isolation, the literature currently lacks a systematic, standardized comparison across multiple medical VLMs for the specific task of CXR report generation^{13,14,15,16}. It is essential to compare model-generated reports under a unified framework and identical experimental conditions.

In this retrospective study, we address this gap by conducting a systematic head-to-head benchmarking of medical image–specific VLMs for CXR report generation. We performed a multidimensional comparison of five recently released models against real-world radiologist-written reference reports, using CXRs obtained from patients presenting to the emergency department.

Materials and Methods

This retrospective study was approved by the Institutional Review Board of Seoul National University Hospital (No. H-2505-199-1646), with a waiver of informed consent.

Patients

Adult patients presenting to the emergency department of a tertiary referral center between January 2022 and April 2025 were retrospectively identified. Eligible patients were those who underwent initial frontal CXR (anteroposterior or posteroanterior view) and chest CT on the same day, with CT serving as the reference standard for finding-level assessment. Among these, patients presenting with fever and/or chills or respiratory symptoms—including dyspnea, cough with or without sputum, blood-tinged sputum or hemoptysis, and chest discomfort or pain—were included. The following patients were excluded: 1) those whose CXR reports contained comparison statements, 2) those whose reports were not available, and 3) those whose reports relied heavily on clinical information rather than imaging findings.

Data Collection

From the electronic medical records, we collected patient demographics, radiologist-written CXR reports, the interval between CXR and CT scan, chief complaints, and comorbidities. Digital Imaging and Communications in Medicine files of CXRs were exported from the Picture Archiving and Communication System. CXRs between January 2022 and February 2024 were primarily interpreted by radiology residents, whereas those between March 2024 and April 2025 were interpreted by board-certified radiologists. The latter period coincided with a nationwide strike by medical students, residents and fellows, which shifted the emergency department workload exclusively to board-certified radiologists^{17,18}.

CXR Report Generation

Five medical image-specific VLMs were employed: AIRead (Soombit.ai, Korea), Lingshu (Alibaba, China), MAIRA-2 (Microsoft Research, UK), MedGemma (Google DeepMind, UK), and MedVersa (Harvard University, MA)^{10,13,14,15,16}. Among these, the latter four models are open-source. For each model, CXR reports were generated from the corresponding Digital Imaging and Communications in Medicine files, without access to clinical information or comparison images. Model inference was performed on a single NVIDIA H100 graphics processing unit running CUDA 12.4, without fine-tuning or transfer learning. Details of each model including their availability are provided in Supplementary Text 1.

Evaluation of VLM-generated CXR Reports

VLM-generated CXR reports were evaluated using two approaches: 1) a multireader study assessing the diagnostic quality of free-text reports based on four criteria (RADPEER score, clinical acceptability, presence of hallucinations, and language clarity)^{10,19}, and 2) finding-level diagnostic sensitivity and specificity.

Report-level Diagnostic Quality

The RADPEER scoring system was originally developed by the American College of Radiology as a peer review tool for quality assurance¹⁹. It uses a three-point scale: a score of 1 indicates complete agreement with the original interpretation, while scores of 2 (understandable miss) and 3 (unacceptable miss) indicate increasing levels of disagreement. Subcategories “a” and “b” further classify findings as clinically insignificant or clinically significant, respectively. The study outcomes were defined as the proportions of reports with a score of 3b (unacceptable, clinically significant miss) and with scores of 2b or 3b combined (any clinically significant miss [i.e., stricter criterion]).

Clinical acceptability was evaluated on a four-point scale that considered the presence of detection errors (e.g., false negatives, false positives, incorrect laterality) and the extent of editing required for clinical use, complementing the RADPEER system¹¹. In this scale, a score of 1 denoted a report that was not acceptable because of detection errors for clinically referable abnormalities. A score of 2 denoted a report acceptable after major revision due to less critical detection errors or the need for extensive edits. A score of 3 denoted a report acceptable only with minor revision, being generally accurate but requiring limited edits. Finally, a score of 4 denoted a report acceptable as is, being accurate, clear, and clinically actionable without edits. The study outcome was the proportion of clinically acceptable reports, defined under two thresholds: 1) the standard criterion, encompassing reports acceptable as is or after minor revision, and 2) the stringent criterion, limited to reports acceptable as is.

Hallucination was defined as the inclusion of information that could not be derived from a single frontal CXR. Examples included references to a lateral view, patient history, comparison studies, or measurements (such as lesion size or distance) not supported by the study setting and models. Language clarity was evaluated as a measure of readability using a five-point scale (1, unacceptable; 2, poor; 3, moderate; 4, good; 5, excellent). The study outcome was the proportion of reports rated 4 or 5.

This evaluation framework was applied to reports generated by the five VLMs as well as to radiologist-written reports. Three board-certified, fellowship-trained thoracic radiologists (J.H.L., 4 years of post-fellowship experience; W.H.L., 2 years; J.Y.L., 1 year) independently evaluated all reports using a web-based assessment platform in a randomized, blinded manner. The criteria are summarized in Supplementary Table 1.

Per-patient Finding-level Analyses

Finding-level sensitivity and specificity were measured for both VLM-generated and radiologist-written CXR reports, with same-day chest CT as the reference. CT scans were reviewed for the presence of predefined abnormalities: aortic aneurysm (≥ 50 mm for the ascending aorta, ≥ 40 mm for the descending

aorta), cardiomegaly (CT cardiothoracic ratio >0.5), cavity, emphysema, hilar mass, lung opacity (consolidation or ground-glass opacity), mediastinal mass, miliary nodules, non-calcified nodule (≥ 4 mm) or mass, pericardial effusion, pleural effusion, pneumomediastinum, pneumoperitoneum, pneumothorax, and reticular opacity^{20,21,22}. Each CT was reviewed by one of three board-certified thoracic radiologists after completion of the reader study.

Then, a previously developed labeler was used to extract the presence or absence of individual findings from the CXR reports (Supplementary Text 2). Briefly, CheXGPT, a Bidirectional Encoder Representations from Transformers-based model trained on 3 million CXR reports was used²³.

Statistical Analyses

The normality of continuous variables was assessed using the Shapiro–Wilk test. Continuous variables were presented as mean \pm standard deviation or as median with interquartile range (IQR), depending on distribution.

The proportions of report quality measures were analyzed using generalized linear mixed-effects models with a logit link. Report source (VLMs or radiologists) was included as a fixed effect, using radiologists as the reference category, while reader and case were modeled as random intercepts. Cases in which original reports contained measurements were excluded from the hallucination analysis. Subgroup analyses were performed, stratified by sex (men vs. women), age (≥ 65 vs. <65 years), and the expertise level of the interpreting radiologist (resident vs. board-certified). For finding-level analyses, sensitivity and specificity with 95% confidence intervals were calculated for each report source and for each abnormality, using CT as the reference standard.

All statistical analyses were performed using R (version 4.1.2) by W.H.L., and a two-sided P value $<.05$ was considered statistically significant.

Results

Patients

Of the 1037 adult patients who presented to the emergency department and underwent initial CXR and CT, the following were excluded: 1) patients without fever, chills, or respiratory symptoms (n=537), 2) patients whose CXR reports contained comparison statements (n=19), 3) patients with missing reports (n=1), and 4) patients whose reports relied heavily on clinical information rather than imaging findings (n=2). A total of 478 patients (median age, 67 years [IQR, 50–78]; 282 men [59.0%]) were included in the final analyses (Fig. 1).

The most common chief complaint was dyspnea (47.7% [228/478]), followed by fever and/or chills (23.6% [113/478]) (Table 1). Malignancy was present in 5.4% (26/478) of patients (lung cancer, n=9; other solid organ malignancy, n=12; hematologic malignancy, n=5), and diffuse parenchymal lung disease was identified in 3.1% (15/478; chronic obstructive pulmonary disease, n=10; interstitial lung disease, n=5) (Table 1).

Report-level Diagnostic Quality

The median word count was 5 words (IQR, 4–7) for radiologists, 10 (IQR, 4–15) for AIRead, 32 (IQR, 27–38) for Lingshu, 19 (IQR, 14–28) for MAIRA-2, 275 (IQR, 242–321) for MedGemma, and 46 (IQR, 32–66) for MedVersa.

The proportion of radiologist-written reports containing RADPEER 3b disagreement was 13.9% (200/1434). Among the VLM-generated reports, compared with radiologists' reports, AIRead showed a lower proportion of RADPEER 3b (5.3% [76/1434], $P<.001$), whereas other VLMs showed higher proportions: Lingshu (43.0% [616/1434], $P<.001$), MAIRA-2 (24.5% [352/1434], $P<.001$), MedGemma (16.8% [241/1434], $P=.02$), and MedVersa (25.9% [371/1434], $P<.001$) (Table 2, Fig. 2A). For RADPEER 2b or 3b disagreement, the proportion was also lower with AIRead compared with radiologists (AIRead, 20.3% [291/1434] vs. radiologists, 30.3% [435/1434]; $P<.001$), but higher with

Lingshu (57.1% [819/1434], $P<.001$), MAIRA-2 (36.8% [528/1434], $P<.001$), and MedVersa (38.4% [551/1434], $P<.001$) (Table 2, Fig. 2A). MedGemma demonstrated RADPEER 2b or 3b rates (27.9% [400/1434], $P=.10$) comparable to those of radiologists.

The proportion of clinically acceptable reports using the standard criterion differed among the VLMs. AIRead showed the highest acceptability, higher than that of radiologists (AIRead, 84.5% [1212/1434] vs. radiologists, 74.3% [1065/1434]; $P<.001$) (Table 2, Fig. 2B). All other models showed lower acceptability than radiologists: Lingshu (41.1% [589/1434]), MAIRA-2 (65.6% [941/1434]), MedGemma (71.4% [1024/1434]), and MedVersa (63.7% [914/1434]) ($P<.05$ for all) (Table 2, Fig. 2B). Under the stringent criterion, AIRead still showed the highest acceptability, which was greater than that of radiologists (58.2% [834/1434] vs. 43.5% [624/1434], $P<.001$) (Table 2, Fig. 2B). MedGemma demonstrated an acceptability rate similar to that of radiologists (42.9% [615/1434], $P=.68$), whereas the other VLM-generated reports showed lower acceptability (25.3–39.7%, $P<.05$ for all).

A single hallucination was identified in the radiologist-written reports, which was not a true hallucination but rather a reviewer's subjective interpretation of a false-positive finding. The proportion of reports containing hallucinations was considerably higher in Lingshu (11.0% [157/1425]), MAIRA-2 (17.4% [248/1425]), MedGemma (5.4% [77/1425]), and MedVersa (12.3% [175/1425]) than in radiologists (0.1% [1/1425], $P<.05$ for all) (Table 2). In contrast, hallucinations were markedly suppressed in AIRead, with only 0.3% of reports (4/1425, $P=.21$) affected.

In terms of language clarity, AIRead (82.9% [1189/1434], $P=.001$), Lingshu (88.0% [1262/1434], $P<.001$), and MedVersa (88.4% [1268/1434], $P<.001$) outperformed radiologists (78.1% [1120/1434]). MedGemma had the lowest proportion of clear language among report sources (69.7% [1000/1434], $P<.001$) (Table 2, Fig. 2C).

These trends remained similar in subgroups stratified by sex, age, and the experience level of the interpreting radiologists (Supplementary Tables 2–7). Representative cases are shown in Figs. 3–5.

Finding-level Diagnostic Performance

The most frequent CT findings were lung opacity (consolidation or ground-glass opacity) in 53.8% (257/478), followed by pleural effusion in 42.3% (202/478), nodule or mass in 23.4% (112/478), emphysema in 18.2% (84/478), and cardiomegaly in 15.7% (75/478) (Tables 3–4).

Per-patient sensitivity and specificity for detecting major abnormalities potentially related to patients' acute symptoms (i.e., lung opacity and pleural effusion) varied across VLMs. AIRead and MedGemma achieved the highest sensitivity for lung opacity and pleural effusion, respectively (AIRead for lung opacity: sensitivity, 77.8% [200/257], specificity, 70.6% [156/221]; MedGemma for pleural effusion: sensitivity, 71.8% [145/202], specificity, 75.0% [207/276]). Lingshu showed the lowest sensitivities for both abnormalities among models (lung opacity: sensitivity, 16.3% [42/257], specificity, 89.1% [197/221]; pleural effusion: sensitivity, 21.3% [43/202], specificity, 90.2% [249/276]). VLMs also exhibited substantial variability for other findings (cardiomegaly: sensitivity, 69.3–86.7% and specificity, 61.5–87.3%; emphysema: sensitivity, 2.4–20.2% and specificity, 94.7–99.2%) (Tables 3–4, Fig. 6).

None of the VLMs identified any of the 10 cases of miliary nodules or the single case of pneumoperitoneum (Tables 3–4, Fig. 6). Lingshu failed to detect any of the nine pneumothorax cases (Table 3, Fig. 6), and AIRead successfully detected the one case of pneumomediastinum (Fig. 5). Additional results are presented in Tables 3–4 and Fig. 6.

Discussion

Although several VLMs for medical imaging have recently been released, comparative evaluations remain limited. In this study, we analyzed CXRs from patients presenting to the emergency department with febrile or respiratory symptoms and compared the performance of five VLMs for report generation against radiologist-written reports acquired from clinical practice. Among the models, AIRead consistently demonstrated the most favorable balance across multiple quality dimensions, achieving lower rates of clinically significant disagreement and higher clinical acceptability, outperforming radiologists. The other VLMs exhibited variable results, with some excelling in language clarity but performing less reliably in diagnostic agreement and/or clinical acceptability. Notably, AIRead demonstrated very low hallucination rates, a desirable feature that enhances report reliability.

A key finding of our work is the discrepancy between diagnostic performance and readability. Fluent, well-structured text does not guarantee clinically accurate or useful content, highlighting that linguistic clarity and diagnostic fidelity are separate dimensions. That is, high language clarity, as observed in Lingshu and MedVersa, did not correspond to greater diagnostic accuracy, whereas MedGemma demonstrated the reverse pattern. MedGemma’s exhaustive and enumerative reporting style performed well under the RADPEER scoring system, which primarily emphasizes report-level agreement; however, this approach appears to compromise readability, thereby limiting its practical utility.

Given that AIRead demonstrated lower rates of clinically significant disagreement (RADPEER 3b), higher acceptability under the stringent criterion, and rare hallucinations, the model may serve as a valuable adjunct in clinical practice. One potential use case is automated draft generation, in which AIRead produces a preliminary report that can be rapidly reviewed and finalized by radiologists, thereby improving efficiency without compromising diagnostic quality. In high-volume or resource-limited settings, AIRead could also function as a second reader to reduce error rates and enhance report consistency. Furthermore, its low hallucination rate suggests potential applicability in emergency or frontline care, where rapid and reliable reporting is essential. These indications

underscore the role of such models not as replacements but as clinical support tools that augment radiologist performance and help maintain reporting quality under heavy workload conditions.

At the finding level, VLMs demonstrated relatively high sensitivities for common abnormalities, including lung opacity, pleural effusion, nodules or masses, and cardiomegaly. However, the reduced specificity observed among some models underscores a trade-off that may lead to false-positive downstream investigations. More critically, both radiologists and VLMs underperformed in detecting rare but clinically relevant findings, such as aortic aneurysms, mediastinal or hilar abnormalities, and pneumoperitoneum. Delayed recognition of these conditions may lead to catastrophic consequences. Therefore, further refinement of VLMs to better identify rare, high-impact abnormalities is essential. It is also important to note that the reference standard for each finding was based on CT results, and the inherent limitations of CXRs in detecting certain abnormalities—such as emphysema, miliary nodules, and pneumoperitoneum—should be considered when interpreting our results, as sensitivities may have been underestimated under these reference standards.

This study has several limitations. First, it was conducted retrospectively at a single institution. Second, CXR reports in Korea are typically written in a concise format, which may limit the generalizability of our findings to countries where more descriptive reporting is standard practice. Third, the diagnostic performance of radiologists in our study may have been underestimated. During the study period, a nationwide strike by medical students, residents, and fellows increased the workload of board-certified radiologists, who had to cover emergency department shifts in addition to their routine clinical duties. This unusual clinical environment may have negatively influenced their performance and should be considered when interpreting the results. Fourth, our evaluation included only one commercial model, with the remainder being open-source, as no other commercial medical image-specific VLMs were available during the study period. Fifth, this study did not assess the downstream impact on patient outcomes. Importantly, improved diagnostic performance does not necessarily translate into favorable clinical outcomes^{24,25}. Sixth, the input to VLMs was limited to images alone, and their performance may be enhanced by incorporating relevant clinical metadata^{26,27}. Finally, this study did not assess human—

AI collaboration, which may further influence the clinical utility of VLM-generated reports.

In conclusion, a few VLMs for CXR report generation are now available, yet our evaluation demonstrated considerable variation in their performance. Among them, one commercial model not only outperformed radiologists in diagnostic quality but also showed an exceptionally low rate of hallucination, which may enhance trust in its outputs.

References

1. Seah, J.C.Y., Tang, J.S.N. & Tran, A. Drafting the Future: The Dawn of AI Report Generation in Radiology. *Radiology*. **316**, 243378; 10.1148/radiol.243378 (2025).
2. Do, K.H., Beck, K.S. & Lee, J.M. The Growing Problem of Radiologist Shortages: Korean Perspective. *Korean J Radiol*. **24**, 1173-1175 (2023).
3. Koo, H.J. & Do, K.H. The Staffing Crisis and Burnout in Academic Radiology: Insights from a Survey Study in Korea. *J Am Coll Radiol*. **21**, 505-514 (2024).
4. Afshari Mirak, S., Tirumani, S.H., Ramaiya, N. & Mohamed, I. The Growing Nationwide Radiologist Shortage: Current Opportunities and Ongoing Challenges for International Medical Graduate Radiologists. *Radiology*. **314**, 232625; 10.1148/radiol.232625 (2025).
5. Zhang, Y. et al. Comparison of Chest Radiograph Captions Based on Natural Language Processing vs Completed by Radiologists. *JAMA Netw Open*. **6**, 2255113; 10.1001/jamanetworkopen.2022.55113 (2023).
6. Nicolson, A., Dowling, J. & Koopman, B. Improving chest X-ray report generation by leveraging warm starting. *Artif Intell Med*. **144**, 102633; 10.1016/j.artmed.2023.102633 (2023).
7. Yu, F. et al. Evaluating progress in automatic chest X-ray radiology report generation. *Patterns (N Y)*. **4**, 100802; 10.1016/j.patter.2023.100802 (2023).
8. Parres, D., Albiol, A. & Paredes, R. Improving Radiology Report Generation Quality and Diversity through Reinforcement Learning and Text Augmentation. *Bioengineering (Basel)*. **11**, 351; 10.3390/bioengineering11040351 (2024).
9. Zambrano Chaves, J.M. et al. A clinically accessible small multimodal radiology model and evaluation metric for chest X-ray findings. *Nat Commun*. **16**, 3108; 10.1038/s41467-025-58344-x (2025).
10. Hong, E.K. et al. Diagnostic Accuracy and Clinical Value of a Domain-specific Multimodal Generative AI Model for Chest Radiograph Report Generation. *Radiology*. **314**, 241476; 10.1148/radiol.241476 (2025).

11. Lee, S., Youn, J., Kim, H., Kim, M. & Yoon, S.H. CXR-LLaVA: a multimodal large language model for interpreting chest X-ray images. *Eur Radiol.* **35**, 4374-4386 (2025)
12. Savage, C.H. et al. Open-Source Large Language Models in Radiology: A Review and Tutorial for Practical Research and Clinical Deployment. *Radiology.* **314**, 241073; 10.1148/radiol.241073 (2025)
13. Xu, W. et al. Lingshu: A Generalist Foundation Model for Unified Multimodal Medical Understanding and Reasoning. *arXiv:2506.07044* <https://arxiv.org/abs/2506.07044> (2025).
14. Bannur, S. et al. MAIRA-2: Grounded Radiology Report Generation. *arXiv:2406.04449* <https://arxiv.org/abs/2406.04449> (2024).
15. Sellergren, A. et al. MedGemma Technical Report. *arXiv:2507.05201* <https://arxiv.org/abs/2507.05201> (2025).
16. Zhou, H.Y. et al. MedVersa: A Generalist Foundation Model for Medical Image Interpretation. *arXiv:2405.07988* <https://arxiv.org/abs/2405.07988> (2024).
17. Park H. Junior doctors' strike in South Korea: systemic barriers undermine medical practice. *BMJ.* **385**, 752; 10.1136/bmj.q752 (2024).
18. de Beer, A., Werner, A.S., Kim, S. & Jenne, F.A. Professional Resistance: Why Korean Medical Students are Boycotting Over Increasing Medical School Places. *Perspect Med Educ.* **13**, 602-607 (2024).
19. Goldberg-Stein, S. et al. ACR RADPEER Committee White Paper with 2016 Updates: Revised Scoring System, New Classifications, Self-Review, and Subspecialized Reports. *J Am Coll Radiol.* **14**, 1080-1086 (2017).
20. Gollub, M.J. et al. Shall we report cardiomegaly at routine computed tomography of the chest? *J Comput Assist Tomogr.* **36**, 67-71 (2012).
21. Munden, R.F. et al. Managing Incidental Findings on Thoracic CT: Mediastinal and Cardiovascular Findings. A White Paper of the ACR Incidental Findings Committee. *J Am Coll Radiol.* **15**, 1087-1096 (2018).
22. Bankier, A.A. et al. Fleischner Society: Glossary of Terms for Thoracic Imaging. *Radiology.* **310**, 232558; 10.1148/radiol.232558 (2024)

23. Hong, E.K. et al. Value of Using a Generative AI Model in Chest Radiography Reporting: A Reader Study. *Radiology*. **314**, 241646; 10.1148/radiol.241646 (2025).
24. Hwang, E.J. & Park, C.M. Clinical Implementation of Deep Learning in Thoracic Radiology: Potential Applications and Challenges. *Korean J Radiol*. **21**, 511-525 (2020).
25. Park, S.H. & Han, K. Methodologic Guide for Evaluating Clinical Performance and Effect of Artificial Intelligence Technology for Medical Diagnosis and Prediction. *Radiology*. **286**, 800-809 (2018).
26. Bluethgen, C. et al. A vision-language foundation model for the generation of realistic chest X-ray images. *Nat Biomed Eng*. **9**, 494-506 (2025).
27. Aksoy, N., Sharoff, S., Baser, S., Ravikumar, N. & Frangi, A.F. Beyond images: an integrative multi-modal approach to chest x-ray report generation. *Front Radiol*. **4**, 1339612 (2024).

Author Contributions

W.H.L. and **J.Y.L.** contributed equally to this work (co-first authorship), particularly in data collection, methodology, and investigation. **J.H.L.** contributed to this work in data collection, and investigation. **S.K.** and **H.K.** contributed equally as senior authors, with primary roles in conceptualization, methodology, resources, software, project administration, and supervision. All contributors have sufficiently participated and meet the criteria for authorship, taking full responsibility for the content of the study. All listed authors have approved the manuscript for submission.

Conflicts of Interests

W.H.L. No relevant relationships.

J.Y.L. No relevant relationships.

J.H.L. received consulting fees from RadiSen; a research grant from Coreline Soft and Kakao Brain, outside of submitted work.

S.K. is the chief technical officer and a shareholder of Soombit.ai.

H.K. Research grants from Kakao Brain and RadiSen, an honorarium from AstraZeneca, consulting fees from RadiSen, stock and stock options in Medical IP, stock in Soombit.ai, and medical director of Soombit.ai.

S.K. is the Chief Technical Officer and a shareholder of Soombit.ai, and **H.K.** is a shareholder of Soombit.ai and serves as its Medical Director. All aspects of data control and analysis were independently performed by W.H.L., who has no conflicts of interest and no affiliation with Soombit.ai. **S.K.** and **H.K.** had no role in data management or analysis.

Funding

Author declared no funding for this work.

Data sharing

Data generated or analyzed during the study are available from the corresponding author by request.

Tables

Table 1: Characteristics of Study Patients

Variable	No. of Patients (n=478)
Age, years*	67 (50–78)
Sex	
Men	282 (59.0)
Women	196 (41.0)
Chest CT-CXR interval, days*	0 (0–0)
Projection	
Posterior-anterior	237 (49.6)
Anterior-posterior	241 (50.4)
Chief complaint	
Fever and/or chill	113 (23.6)
Dyspnea	228 (47.7)
Cough and/or sputum	43 (9.0)
Blood-tinged sputum or hemoptysis	32 (6.7)
Chest discomfort or pain	62 (13.0)
Comorbidity	
Lung cancer	9 (1.9)
Other solid organ malignancy	12 (2.5)
Hematologic malignancy	5 (1.0)
Chronic obstructive pulmonary disease	10 (2.1)
Interstitial lung disease	5 (1.0)
Heart failure	12 (2.5)
Hypertension	156 (32.6)
Diabetes mellitus	94 (19.7)
Stroke	15 (3.1)
Coronary artery disease	17 (3.6)

Data are presented as number of patients (percentage), unless otherwise specified.

*Data are presented as medians (interquartile range).

CT = computed tomography, CXR = chest radiograph.

Table 2: Evaluation of Radiologist-Written and AI-Generated Reports by Three Thoracic Radiologists

Variable	Radiologist	AIRead	Lingshu	MAIRA-2	MedGemma	MedVersa
RADPEER Score 3b, %	13.9 (200/1434)	5.3 (76/1434)	43.0 (616/1434)	24.5 (352/1434)	16.8 (241/1434)	25.9 (371/1434)
P Value	Reference	<.001	<.001	<.001	.02	<.001
RADPEER Score 2b or 3b, %	30.3 (435/1434)	20.3 (291/1434)	57.1 (819/1434)	36.8 (528/1434)	27.9 (400/1434)	38.4 (551/1434)
P Value	Reference	<.001	<.001	<.001	.10	<.001
Clinically Acceptable Reports by Standard Criterion, %	74.3 (1065/1434)	84.5 (1212/1434)	41.1 (589/1434)	65.6 (941/1434)	71.4 (1024/1434)	63.7 (914/1434)
P Value	Reference	<.001	<.001	<.001	.04	<.001
Clinically Acceptable Reports by Stringent Criterion, %	43.5 (624/1434)	58.2 (834/1434)	25.3 (363/1434)	37.3 (535/1434)	42.9 (615/1434)	39.7 (570/1434)
P Value	Reference	<.001	<.001	<.001	.68	.01
Hallucination, %*	0.1 (1/1425)	0.3 (4/1425)	11.0 (157/1425)	17.4 (248/1425)	5.4 (77/1425)	12.3 (175/1425)
P Value	Reference	.21	<.001	<.001	<.001	<.001
Clarity of Language, %	78.1 (1120/1434)	82.9 (1189/1434)	88.0 (1262/1434)	78.4 (1124/1434)	69.7 (1000/1434)	88.4 (1268/1434)
P Value	Reference	.001	<.001	.85	<.001	<.001

Clinical acceptability was defined as “acceptable as is” or “with minor revision” (standard), and strictly as “acceptable as is” only (stringent).

Clarity of language was defined as a score of 4 or higher (good to excellent).

P values represent comparisons against the radiologist as the reference.

*Three patients whose original reports contained measurements were excluded from the analysis of hallucinations.

Table 3: Diagnostic Performance with Chest CT as the Reference Standard

	Radiologist		AIRead		Lingshu	
Findings	Sensitivity, %	Specificity, %	Sensitivity, %	Specificity, %	Sensitivity, %	Specificity, %
Aortic aneurysm	0 (0, 41.0) [0/7]	100 (99.2, 100) [471/471]	28.6 (3.7, 71.0) [2/7]	98.1 (96.3, 99.1) [462/471]	0 (0, 41.0) [0/7]	100 (99.2, 100) [471/471]
Cardiomegaly	21.3 (13.0, 32.6) [16/75]	98.3 (96.3, 99.2) [396/403]	86.7 (76.4, 93.1) [65/75]	77.9 (73.5, 81.8) [314/403]	86.7 (76.4, 93.1) [65/75]	61.5 (56.6, 66.3) [248/403]
Cavity	20 (4.3, 48.1) [3/15]	100 (99.2, 100) [463/463]	6.7 (0.2, 31.9) [1/15]	100 (99.2, 100) [463/463]	0 (0, 21.8) [0/15]	100 (99.2, 100) [463/463]
Emphysema	6.0 (2.2, 14.0) [5/84]	100 (99.1, 100) [394/394]	15.5 (8.8, 25.4) [13/84]	99.2 (97.8, 99.8) [391/394]	2.4 (0.3, 8.3) [2/84]	95.7 (93.0, 97.4) [377/394]
Hilar enlargement	30 (6.7, 65.2) [3/10]	99.1 (97.8, 99.8) [464/468]	80 (44.4, 97.5) [8/10]	94.7 (92.1, 96.4) [443/468]	0 (0, 30.8) [0/10]	98.9 (97.4, 99.6) [463/468]
Lung opacity (consolidation or GGO)	60.7 (54.4, 66.7) [156/257]	85.1 (79.5, 89.4) [188/221]	77.8 (72.1, 82.6) [200/257]	70.6 (64.0, 76.4) [156/221]	16.3 (12.2, 21.6) [42/257]	89.1 (84.1, 92.8) [197/221]
Mediastinal widening	21.1 (6.1, 45.6) [4/19]	99.3 (98.1, 99.9) [456/459]	57.9 (33.5, 79.7) [11/19]	99.1 (97.8, 99.8) [455/459]	15.8 (3.4, 39.6) [3/19]	85.4 (81.8, 88.4) [392/459]
Miliary nodule	0 (0, 30.8) [0/10]	100 (99.2, 100) [468/468]	0 (0, 30.8) [0/10]	100 (99.2, 100) [468/468]	0 (0, 30.8) [0/10]	100 (99.2, 100) [468/468]
Nodule or mass	20.5 (13.7, 29.4) [23/112]	97.0 (94.5, 98.4) [355/366]	36.6 (27.9, 46.3) [41/112]	87.4 (83.5, 90.6) [320/366]	0.9 (0, 4.9) [1/112]	99.5 (98.0, 99.9) [364/366]
Pericardial effusion	0 (0, 6.1) [0/59]	100 (99.1, 100) [419/419]	0 (0, 6.1) [0/59]	100 (99.1, 100) [419/419]	0 (0, 6.1) [0/59]	100 (99.1, 100) [419/419]
Pleural effusion	43.1 (36.2, 50.2) [87/202]	97.5 (94.6, 98.9) [269/276]	68.3 (61.4, 74.6) [138/202]	92.0 (88.0, 94.8) [254/276]	21.3 (16.0, 27.7) [43/202]	90.2 (85.9, 93.3) [249/276]
Pneumomediastinum	100 (2.5, 100) [1/1]	100 (99.2, 100) [477/477]	100 (2.5, 100) [1/1]	100 (99.2, 100) [477/477]	0 (0, 97.5) [0/1]	100 (99.2, 100) [477/477]
Pneumoperitoneum	0 (0, 97.5) [0/1]	100 (99.2, 100) [477/477]	0 (0, 97.5) [0/1]	99.8 (98.8, 100) [476/477]	0 (0, 97.5) [0/1]	100 (99.2, 100) [477/477]

Pneumothorax	77.8 (40.0, 97.2) [7/9]	99.8 (98.8, 100) [468/469]	77.8 (40.0, 97.2) [7/9]	100 (99.2, 100) [469/469]	0 (0, 33.6) [0/9]	99.6 (98.5, 99.9) [467/469]
Reticular opacity	7.1 (0.9, 23.5) [2/28]	98.4 (96.7, 99.3) [443/450]	25.0 (10.7, 44.9) [7/28]	99.8 (98.8, 100) [449/450]	3.6 (0.1, 18.3) [1/28]	95.6 (93.1, 97.2) [430/450]

Values in parentheses indicate 95% confidence intervals, and data in brackets denote numerators and denominators.

GGO = ground-glass opacity.

Table 4: Diagnostic Performance with Chest CT as the Reference Standard

	MAIRA-2		MedGemma		MedVersa	
Findings	Sensitivity,	Specificity,	Sensitivity,	Specificity,	Sensitivity,	Specificity,
Aortic aneurysm	0 (0, 41.0) [0/7]	100 (99.2, 100) [471/471]	0 (0, 41.0) [0/7]	100 (99.2, 100) [471/471]	0 (0, 41.0) [0/7]	100 (99.2, 100) [471/471]
Cardiomegaly	72.0 (60.3, 81.5) [54/75]	85.6 (81.7, 88.8) [345/403]	73.3 (61.7, 82.6) [55/75]	81.1 (76.9, 84.8) [327/403]	69.3 (57.5, 79.2) [52/75]	87.3 (83.6, 90.4) [352/403]
Cavity	0 (0, 21.8) [0/15]	99.8 (98.8, 100) [462/463]	0 (0, 21.8) [0/15]	99.6 (98.4, 99.9) [461/463]	0 (0, 21.8) [0/15]	100 (99.2, 100) [463/463]
Emphysema	6.0 (2.2, 14.0) [5/84]	98.2 (96.2, 99.2) [387/394]	4.8 (1.3, 11.7) [4/84]	97.5 (95.2, 98.7) [384/394]	20.2 (12.6, 30.7) [17/84]	94.7 (91.8, 96.6) [373/394]
Hilar enlargement	20 (2.5, 55.6) [2/10]	96.8 (94.6, 98.1) [453/468]	10 (0.3, 44.5) [1/10]	96.2 (93.9, 97.6) [450/468]	10 (0.3, 44.5) [1/10]	98.3 (96.5, 99.2) [460/468]
Lung opacity (consolidation or GGO)	51.4 (45.1, 57.6) [132/257]	82.8 (77.0, 87.4) [183/221]	76.7 (70.9, 81.6) [197/257]	47.5 (40.8, 54.3) [105/221]	39.3 (33.3, 45.6) [101/257]	86.9 (81.5, 90.9) [192/221]
Mediastinal widening	5.3 (0.1, 26.0) [1/19]	99.3 (98.1, 99.9) [456/459]	15.8 (3.4, 39.6) [3/19]	95.6 (93.2, 97.2) [439/459]	10.5 (1.3, 33.1) [2/19]	99.6 (98.4, 99.9) [457/459]
Miliary nodule	0 (0, 30.8) [0/10]	100 (99.2, 100) [468/468]	0 (0, 30.8) [0/10]	100 (99.2, 100) [468/468]	0 (0, 30.8) [0/10]	100 (99.2, 100) [468/468]
Nodule or mass	7.1 (3.4, 14.0) [8/112]	98.1 (95.9, 99.2) [359/366]	26.8 (19.1, 36.1) [30/112]	82.8 (78.4, 86.4) [303/366]	3.6 (1.0, 8.9) [4/112]	98.4 (96.3, 99.3) [360/366]
Pericardial effusion	0 (0, 6.1) [0/59]	100 (99.1, 100) [419/419]	5.1 (1.1, 14.1) [3/59]	98.1 (96.1, 99.1) [411/419]	0 (0, 6.1) [0/59]	100 (99.1, 100) [419/419]
Pleural effusion	43.6 (36.7, 50.7) [88/202]	91.3 (87.2, 94.2) [252/276]	71.8 (65.0, 77.8) [145/202]	75.0 (69.4, 79.9) [207/276]	48.0 (41.0, 55.1) [97/202]	97.1 (94.2, 98.6) [268/276]
Pneumomediastinum	0 (0, 97.5) [0/1]	100 (99.2, 100) [477/477]	0 (0, 97.5) [0/1]	100 (99.2, 100) [477/477]	0 (0, 97.5) [0/1]	100 (99.2, 100) [477/477]
Pneumoperitoneum	0 (0, 97.5) [0/1]	100 (99.2, 100) [477/477]	0 (0, 97.5) [0/1]	100 (99.2, 100) [477/477]	0 (0, 97.5) [0/1]	100 (99.2, 100) [477/477]

Pneumothorax	55.6 (21.2, 86.3) [5/9]	99.6 (98.5, 99.9) [467/469]	22.2 (2.8, 60.0) [2/9]	98.1 (96.3, 99.1) [460/469]	44.4 (13.7, 78.8) [4/9]	99.4 (98.1, 99.9) [466/469]
Reticular opacity	7.1 (0.9, 23.5) [2/28]	99.1 (97.7, 99.8) [446/450]	28.6 (13.2, 48.7) [8/28]	93.1 (90.3, 95.2) [419/450]	28.6 (13.2, 48.7) [8/28]	95.6 (93.1, 97.2) [430/450]

Values in parentheses indicate 95% confidence intervals, and data in brackets denote numerators and denominators.

GGO = ground-glass opacity.

Figure Legends

Figure 1: Flow diagram of patient inclusion and exclusion.

Figure 2: Comparative evaluation of chest radiograph reports generated by vision–language models against real-world radiologist-written reports.

All chest radiograph reports were independently reviewed and rated in a blinded and randomized manner by three thoracic radiologists.

(A) Distribution of RADPEER scores across five vision–language models (AIRead, Lingshu, MAIRA-2, MedGemma, and MedVersa) and radiologists (i.e., original reports). RADPEER categories indicate levels of interpretive agreement, with lower scores reflecting higher agreement and higher scores reflecting greater discrepancies. Within each score, the “a” descriptor denotes a clinically insignificant discrepancy, whereas “b” denotes a clinically significant one.

(B) Clinical acceptability of reports, categorized as acceptable as is, acceptable with minor revision, acceptable only with major revision, or not acceptable.

(C) Clarity of language scored on a 5-point scale with higher scores representing greater clarity.

Figure 3: Representative chest radiographs and reports of true-positive cases.

(A) A 74-year-old woman with dyspnea. Frontal chest radiograph shows multifocal patchy ground-glass opacities and consolidation, predominantly in the right lung, with bilateral costophrenic angle blunting suggestive of bilateral pleural effusion. CT confirmed corresponding abnormalities. All report sources appropriately detected lung opacity (with variable terminology); however, bilateral pleural effusion was missed in some reports (radiologist, Lingshu, MedVersa). Green=true positive/true negative; red=false positive/false negative.

(B) A 79-year-old man with dyspnea. Frontal chest radiograph shows increased pulmonary vascularity with equivocal peribronchial opacities; CT confirmed interlobular septal thickening. Some report sources suggested pulmonary congestion/edema, whereas MAIRA-2 and MedVersa failed to report

these findings. Green=true positive/true negative; red=false positive/false negative.

Figure 4: Representative chest radiographs and reports of false-positive cases.

(A) A 35-year-old man with chest discomfort. Radiograph demonstrates left pleural effusion and cardiomegaly; CT confirmed pericardial effusion with pericardial thickening and left pleural effusion. AIRead and MedVersa correctly described these findings, whereas others partially or entirely missed them. MedVersa falsely reported a pneumothorax, and Lingshu generated comparison statements. Green=true positive/true negative; red=false positive/false negative; yellow=hallucination.

(B) A 66-year-old woman with fever. Chest radiograph was interpreted as normal by all readers; CT revealed subtle bilateral ground-glass opacities, suggestive of atypical pneumonia. Lingshu reported endotracheal intubation, which was a false positive. Green=true positive/true negative; red=false positive/false negative; yellow=hallucination.

Figure 5: Representative chest radiographs and reports illustrating hallucinations and issues of language clarity.

(A) A 29-year-old man with chest discomfort. Radiograph and CT showed pneumomediastinum and subcutaneous emphysema. Radiologist and AIRead reports were appropriate, whereas MAIRA-2 included comparison statements and MedGemma inferred medical information. Green=true positive/true negative; red=false positive/false negative; yellow=hallucination.

(B) A 26-year-old man with chest pain and pneumothorax. Lingshu failed to report the large right pneumothorax, while other models described it correctly. MedVersa included a hallucinated statement regarding physician communication. Notably, MedGemma employed an enumerative manner, incorrectly characterizing the obvious compressive atelectasis caused by a large pneumothorax as mass/tumor, infection, fluid, or consolidation, thereby obscuring language clarity. Additionally, MedGemma's reports sometimes contained incomplete sentences. Green=true positive/true negative; red=false positive/false negative; yellow=hallucination/poor language clarity; underline=incomplete sentence.

Figure 6: Sensitivity and specificity for individual findings.

Forest plots show the sensitivity (left) and specificity (right) with 95% confidence intervals for 15 findings, including cardiomegaly, consolidation or ground-glass opacity (GGO), pleural effusion, pneumothorax, pneumomediastinum, hilar enlargement, mediastinal widening, reticular opacity, nodule or mass, emphysema, aortic aneurysm, cavity, pericardial effusion, miliary nodule, and pneumoperitoneum. Results are compared across five vision–language models (AIRead, Lingshu, MAIRA-2, MedGemma, and MedVersa) and radiologists (i.e., original reports).

Figures

Figure 1: Flow diagram of patient inclusion and exclusion.

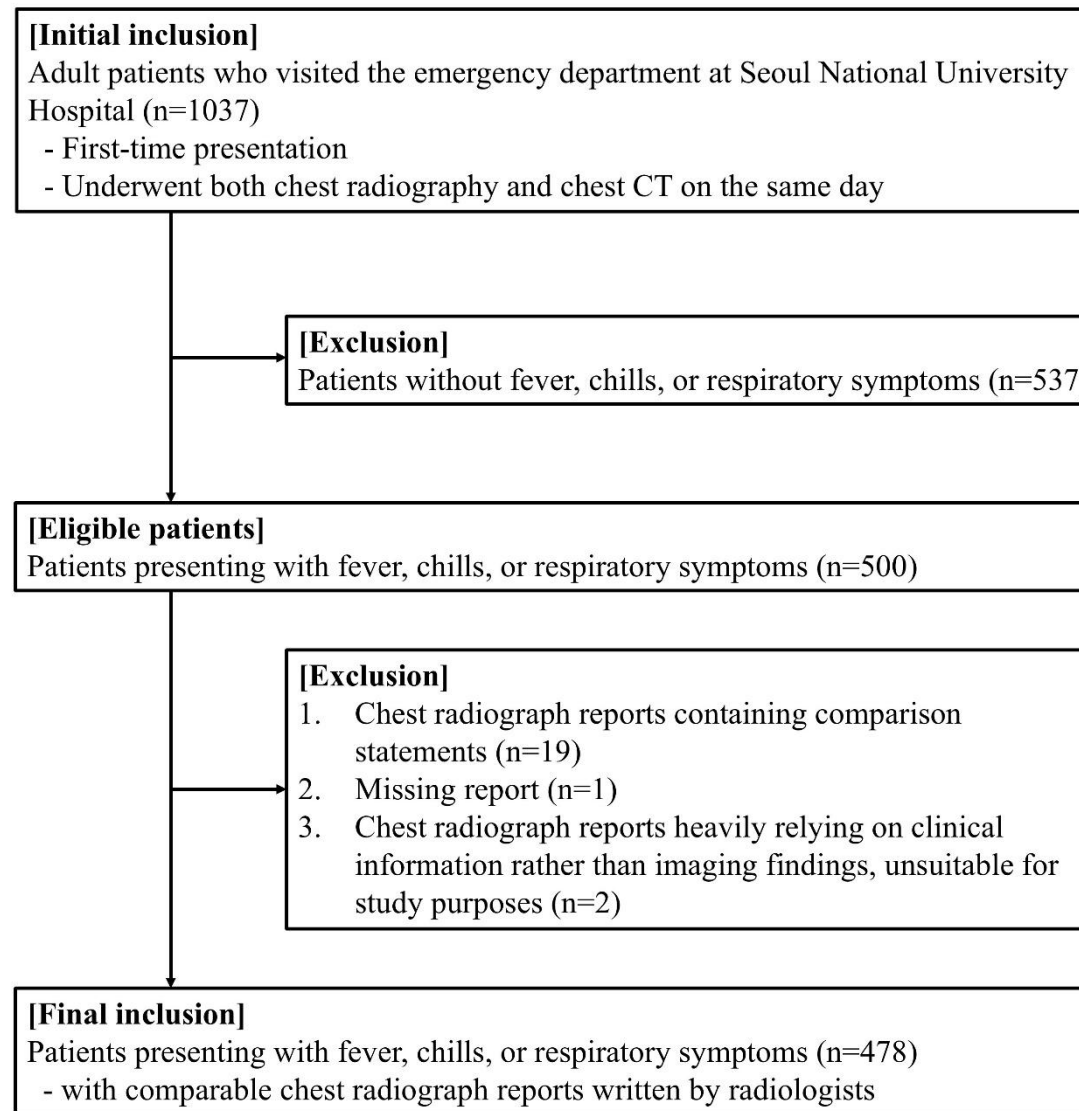
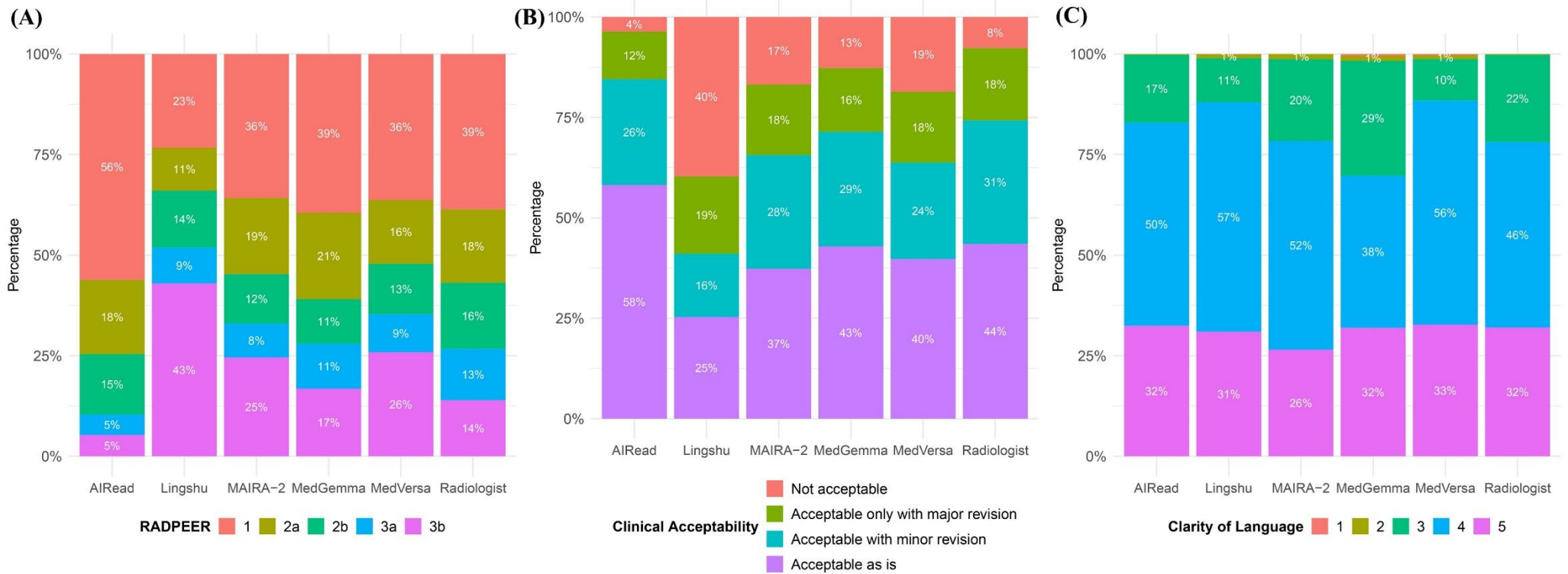


Figure 2: Comparative evaluation of chest radiograph reports generated by vision–language models against real-world radiologist-written reports.



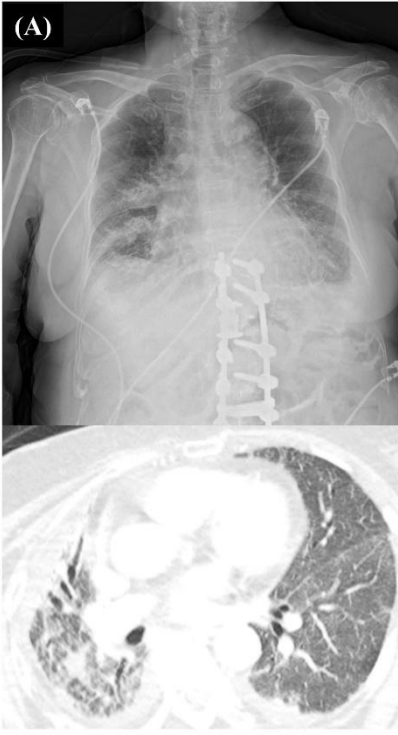

All chest radiograph reports were independently reviewed and rated in a blinded and randomized manner by three thoracic radiologists.

(A) Distribution of RADPEER scores across five vision–language models (AIRead, Lingshu, MAIRA-2, MedGemma, and MedVersa) and radiologists (i.e., original reports). RADPEER categories indicate levels of interpretive agreement, with lower scores reflecting higher agreement and higher scores reflecting greater discrepancies. Within each score, the “a” descriptor denotes a clinically insignificant discrepancy, whereas “b” denotes a clinically significant one.

(B) Clinical acceptability of reports, categorized as acceptable as is, acceptable with minor revision, acceptable only with major revision, or not acceptable.

(C) Clarity of language scored on a 5-point scale with higher scores representing greater clarity.

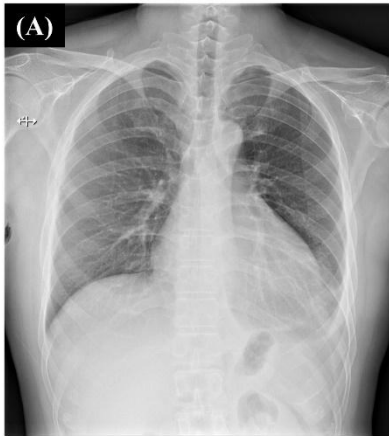

Figure 3: Representative chest radiographs and reports of true-positive cases.

<p>(A)</p>  <p>Radiologist: Diffuse haziness in both lungs. Consolidation in Rt. lung.</p>	<p>Lingshu: Findings: The heart is normal in size. There is no mediastinal widening. Diffuse bilateral airspace opacities are present. No large pleural effusion or pneumothorax. Impression: Bilateral airspace opacities may reflect pulmonary edema or infection.</p>	<p>MedVersa: Findings: Single supine AP portable view of the chest was obtained. There are diffuse bilateral pulmonary opacities, right greater than left, with differential diagnosis including pulmonary hemorrhage, pulmonary contusion, infection, or asymmetric pulmonary edema. No large pleural effusion is seen. There is no evidence of pneumothorax. The cardiac silhouette is not enlarged. Mediastinal contours are unremarkable. Impression: Diffuse bilateral pulmonary opacities with differential diagnosis including pulmonary hemorrhage, pulmonary contusion, infection, or asymmetric pulmonary edema. No large pleural effusion. No evidence of pneumothorax.</p>
	<p>MAIRA-2: PA AP chest demonstrates cardiomegaly. Bilateral infiltrates are observed right greater than left. There is a right pleural effusion.</p> <p>AIRead: Pulmonary edema with both pleural effusion. DDx. combined pneumonic infiltration.</p>	
<p>(B)</p>  <p>Radiologist: cardiomegaly increased pulmonary vascularity suspicious retrocardiac increased opacity in right thorax. - ddx) mass, pseudolesion by bronchial opacity reC) consider chest CT</p>	<p>Lingshu: Findings: The heart is mildly enlarged. There is pulmonary vascular redistribution with hazy ill-defined vascularity. There is also bilateral basilar alveolar infiltrate. Impression: CHF.</p> <p>MAIRA-2: PA AP chest demonstrates cardiomegaly. Lungs are clear.</p>	<p>MedVersa: Findings: The heart is mildly enlarged. The aorta is mildly tortuous. There is no pleural effusion or pneumothorax. The lungs appear clear. Impression: No evidence of acute cardiopulmonary disease.</p> <p>AIRead: Cardiomegaly with aortic calcification. R/O mild pulmonary edema.</p>
	<p>MedGemma: Okay, here's a description of the chest X-ray based on the image you provided: **Overall Impression:** The chest X-ray shows a moderately enlarged heart (cardiomegaly) and some evidence of pulmonary vascular congestion. The lung fields appear relatively clear, but there are some subtle findings that warrant further consideration. **Specific Findings:** * Cardiomegaly: The heart appears enlarged, which could be due to various causes such as hypertension, coronary artery disease, valvular heart disease, or cardiomyopathy. The degree of enlargement is moderate. * Pulmonary Vascular Congestion: There is some increased prominence of the pulmonary vessels, suggesting increased blood flow to the lungs. This could be due to heart failure, pulmonary hypertension, or other conditions that increase the workload of the heart. * Lung Fields: The lung fields appear relatively clear, with no obvious consolidation (areas of dense opacity suggesting pneumonia or other infection). There is no evidence of significant pleural effusion (fluid in the pleural space). * Bones: The bony structures of the ribs and clavicles appear intact. * Mediastinum: The mediastinum (the space between the lungs containing the heart, great vessels, trachea, and esophagus) appears within normal limits. * Diaphragm: The diaphragms are seen, but the image quality is not ideal for detailed assessment. **Possible Considerations:** * Differential Diagnosis: Given the findings, the differential diagnosis includes heart failure, hypertension, coronary artery disease, valvular heart disease, cardiomyopathy, and other conditions that can cause cardiomegaly and pulmonary vascular congestion. * Further Evaluation: Depending on the clinical context and the patient's symptoms, further evaluation may be warranted, such as an echocardiogram to assess cardiac function, blood tests to evaluate for heart failure markers, or other imaging studies. **Disclaimer:** This is a preliminary interpretation based on a single image. A definitive diagnosis requires a complete clinical evaluation, including the patient's history, physical examination findings, and other relevant investigations. This interpretation should not be used to make any medical decisions without consulting a qualified healthcare professional.</p>	

(A) A 74-year-old woman with dyspnea. Frontal chest radiograph shows multifocal patchy ground-glass opacities and consolidation, predominantly in the right lung, with bilateral costophrenic angle blunting suggestive of bilateral pleural effusion. CT confirmed corresponding abnormalities. All report sources appropriately detected lung opacity (with variable terminology); however, bilateral pleural effusion was missed in some reports (radiologist, Lingshu, MedVersa). Green=true positive/true negative; red=false positive/false negative.

(B) A 79-year-old man with dyspnea. Frontal chest radiograph shows increased pulmonary vascularity with equivocal peribronchial opacities; CT confirmed interlobular septal thickening. Some report sources suggested pulmonary congestion/edema, whereas MAIRA-2 and MedVersa failed to report these findings. Green=true positive/true negative; red=false positive/false negative.

Figure 4: Representative chest radiographs and reports of false-positive cases.

Radiologist:
Grossly no active lung lesion

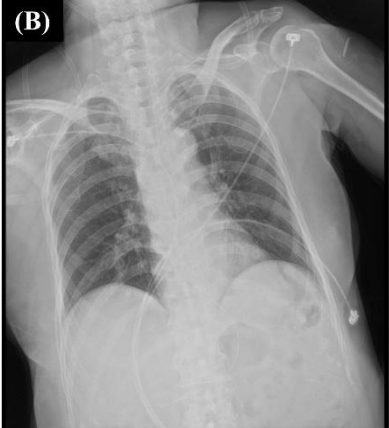

Lingshu:
Findings:
The heart is mildly enlarged.
The mediastinal and hilar contours appear unchanged.
There is no pleural effusion or pneumothorax.
The lungs appear clear.
Impression:
No evidence of acute disease.

MedVersa:
Findings:
The heart is mildly enlarged. The mediastinal and hilar contours appear within normal limits. There is a small to moderate left-sided pleural effusion with a small left-sided pneumothorax. The lungs appear clear.
Impression:
Small to moderate left-sided pleural effusion with a small left-sided pneumothorax.

MAIRA-2:
Cardiomediastinal contours are within normal limits for technique. Small left pleural effusion is present with adjacent focus of atelectasis or consolidation. Right lung and pleural surfaces are clear.

AIRead:
Heart is slightly enlarged.
Left pleural effusion.

MedGemma:
Okay, here's a description of the chest X-ray based on the image provided:
****Overall Impression:****
The image shows a standard PA (Posterior-Anterior) chest X-ray. The heart size appears to be mildly enlarged. There is a possible opacity in the left lower lung field.
****Detailed Findings:****
* ****Heart Size:**** The heart appears to be mildly enlarged, with a slightly increased cardiothoracic ratio (CTR). The CTR is typically considered normal when it's less than 0.5. In this case, the CTR is likely slightly above 0.5.
* ****Lung Fields:**** The lung fields appear relatively clear, with no obvious signs of consolidation, pneumothorax, or large pleural effusions.
* ****Mediastinum:**** The mediastinum (the space between the lungs containing the heart, great vessels, trachea, etc.) appears within normal limits in terms of width and contour.
* ****Bones:**** The ribs and clavicles appear intact.
* ****Left Lower Lung Field:**** There is a possible opacity in the left lower lung field. This could be due to a variety of factors, including atelectasis (lung collapse), consolidation (infection), or a mass. Further evaluation with a CT scan may be warranted to determine the cause.
****Important Considerations:****
* This is a single image, and a complete assessment requires reviewing the entire X-ray, including the lateral view (if available).
* The interpretation is based solely on the provided image. Clinical history and physical examination findings are essential for a comprehensive diagnosis.
* The possible opacity in the left lower lung field requires further investigation.
****Disclaimer:****
This is a preliminary interpretation based on a single image. A definitive diagnosis requires a complete clinical evaluation and potentially additional imaging studies. This information is not intended to be a substitute for professional medical advice.

Radiologist:
No active lung lesion.

Lingshu:
Findings:
The endotracheal tube is 4 cm above the carina. There is no focal consolidation or pneumothorax. There is mild cardiomegaly.
Impression:
No acute cardiopulmonary process.

MedVersa:
Findings:
The lungs are clear without focal consolidation. No pleural effusion or pneumothorax is seen. The cardiac and mediastinal silhouettes are unremarkable. No displaced fracture is seen.
Impression:
No acute cardiopulmonary process.

MAIRA-2:
PA AP chest demonstrates normal heart size. Lungs are clear. NG tube overlies the stomach.

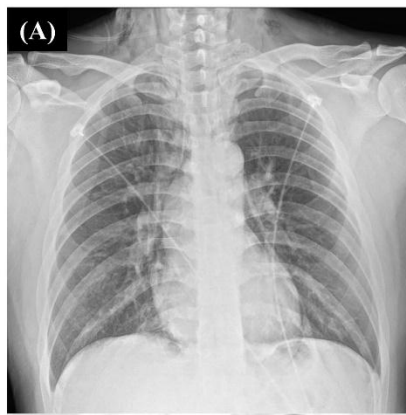
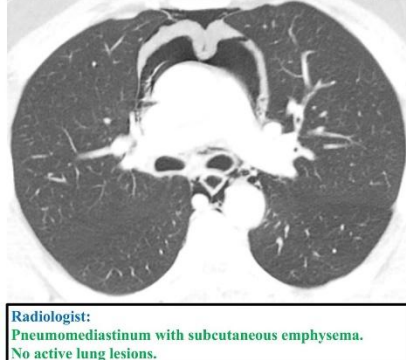


AIRead:
CVC, NG tube insertion state.
Aortic calcification.

MedGemma:
Okay, here's a description of the X-ray based on the image provided:
****General Impression:****
The image shows a chest X-ray with several lines and tubes visible. The patient is likely in a hospital setting, given the presence of medical devices.
****Key Findings:****
* ****Lines and Tubes:**** There are multiple lines and tubes visible within the chest. These likely represent:
* ****Central Venous Catheter (CVC):** A catheter is seen entering the right subclavian vein.
* ****Nasogastric Tube (NG Tube):** An NG tube is visible, likely terminating in the stomach.
* ****Other lines:** There are other lines that are not easily identified, but they are likely related to medical monitoring or treatment.
* ****Bones:** The ribs, clavicles, and humeri are visible. There are no obvious fractures or dislocations.
* ****Lungs:** The lungs appear relatively clear, with no obvious consolidation, effusions, or pneumothorax. However, the image quality is somewhat limited by the presence of the lines and tubes, which can obscure the lung fields.
* ****Heart and Mediastinum:** The heart size appears within normal limits. The mediastinum (the space between the lungs containing the heart, great vessels, trachea, etc.) appears unremarkable.
* ****Abdomen:** The abdominal structures are visible, but the image quality is not ideal for detailed assessment.
****Limitations:****
* ****Image Quality:** The presence of multiple lines and tubes obscures the lung fields, making it difficult to assess for subtle abnormalities.
* ****Patient Positioning:** The patient's position may not be optimal for a standard chest X-ray.
****Overall:****
This X-ray shows a chest with several medical lines and tubes present. The lungs appear relatively clear, but the image quality is limited. Further evaluation may be needed to assess for any subtle abnormalities.
****Disclaimer:**** This is a preliminary interpretation based on a single image. A complete evaluation requires a full clinical history, physical examination, and potentially additional imaging studies.

(A) A 35-year-old man with chest discomfort. Radiograph demonstrates left pleural effusion and cardiomegaly; CT confirmed pericardial effusion with pericardial thickening and left pleural effusion. AIRead and MedVersa correctly described these findings, whereas others partially or entirely missed them. MedVersa falsely reported a pneumothorax, and Lingshu generated comparison statements. Green=true positive/true negative; red=false positive/false negative; yellow=hallucination.

(B) A 66-year-old woman with fever. Chest radiograph was interpreted as normal by all readers; CT revealed subtle bilateral ground-glass opacities, suggestive of atypical pneumonia. Lingshu reported endotracheal intubation, which was a false positive. Green=true positive/true negative; red=false positive/false negative; yellow=hallucination.

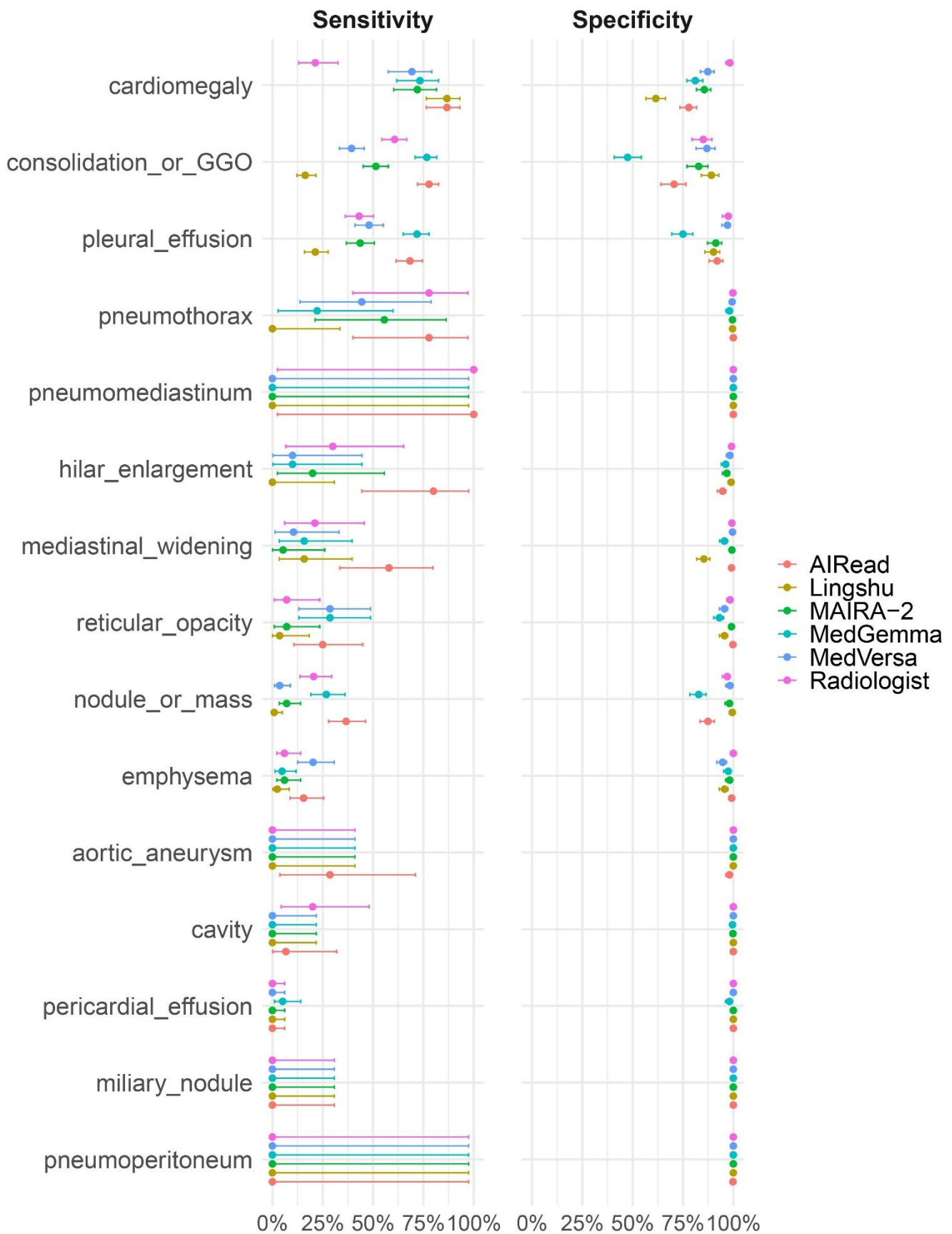
Figure 5: Representative chest radiographs and reports illustrating hallucinations and issues of language clarity.

<p>(A)</p> 	<p>Lingshu: Findings: The heart is normal in size. The mediastinum is unremarkable. The lungs are clear. Impression: No acute disease.</p>	<p>MedVersa: Findings: The lungs are clear. Cardiac silhouette is normal in size. There is no pleural effusion, pneumothorax or pulmonary edema. There is extensive subcutaneous emphysema. There is no free air under the diaphragm. Impression: Extensive subcutaneous emphysema without evidence of pneumomediastinum or pneumothorax. No acute cardiopulmonary process.</p>
	<p>MAIRA-2: Right chest tube has been removed. There is a small residual right apical pneumothorax. There is no evidence of mediastinal shift. No focal infiltrates are seen.</p>	<p>AIRead: Pneumomediastinum. Subcutaneous emphysema.</p>
<p>Radiologist: Pneumomediastinum with subcutaneous emphysema. No active lung lesions.</p>	<p>MedGemma: Okay, here's a description of the chest X-ray based on the image provided: **Overall Impression:** The image shows a chest X-ray with the patient likely intubated and potentially sedated. The presence of lines and tubes suggests a hospital setting. **Key Findings:** * **Bones:** The ribs, clavicles, and scapulae are visible. There are no obvious fractures or dislocations. * **Lungs:** The lungs appear relatively clear, with no obvious consolidation, effusions, or pneumothorax. However, the visualization of the lung parenchyma is limited due to the presence of the lines and tubes. * **Heart:** The heart size appears within normal limits. * **Mediastinum:** The mediastinum (the space between the lungs containing the heart, great vessels, trachea, etc.) appears unremarkable. * **Lines and Tubes:** There are several lines and tubes present, including: * **Endotracheal Tube (ETT):** The ETT is visible in the trachea, likely in place to secure the patient's airway. * **Central Venous Catheter (CVC):** A CVC is visible, likely in the superior vena cava. * **Other lines:** There are other lines that are not clearly identified. **Limitations:** * **Limited Lung Visualization:** The presence of the lines and tubes obscures the visualization of the lung parenchyma, making it difficult to assess for subtle abnormalities. * **Patient Positioning:** The patient's position may not be ideal for optimal visualization of the chest. **In summary,** this chest X-ray shows a patient with lines and tubes in place, likely intubated. The lungs appear relatively clear, but the visualization is limited. Further evaluation may be needed to assess for any underlying pathology. **Disclaimer:** This is a preliminary interpretation based on a single image. A complete evaluation requires clinical correlation and potentially additional imaging.</p>	
<p>(B)</p> 	<p>Lingshu: Findings: The heart is normal in size. The mediastinal and hilar contours appear within normal limits. There is no pleural effusion or pneumothorax. The lungs appear clear. Impression: No evidence of acute cardiopulmonary disease.</p>	<p>MedVersa: Findings: There is a large right pneumothorax with near complete collapse of the right lung. The left lung is clear. The heart size is normal. There is no pleural effusion. Impression: Large right pneumothorax with near complete collapse of the right lung. Recommend chest tube placement. These findings were discussed with Dr. _____ by Dr. _____ at 11:35 a.m. on _____ by telephone.</p>
	<p>AIRead: Right pneumothorax.</p>	<p>MedGemma: Okay, here's a description of the chest X-ray based on the image provided: **Overall Impression:** The X-ray shows a significant abnormality in the right hemithorax (right side of the chest). There appears to be a large opacity or mass occupying a significant portion of the right lung field. The left lung appears relatively clear. **Specific Findings:** * **Right Hemithorax Opacity:** The most striking feature is the dense opacity in the right lung. This could be due to a variety of causes, including: * **Mass/Tumor:** A primary lung tumor or metastasis from another site. * **Infection:** Pneumonia, abscess, or other infectious process. * **Fluid:** Pleural effusion (fluid in the pleural space) or hemothorax (blood in the pleural space). * **Consolidation:** Lung consolidation due to infection or other inflammatory process. * **Atelectasis:** Collapse of the lung. * **Left Lung:** The left lung appears relatively clear, with normal lung markings. * **Mediastinum:** The mediastinum (the space between the lungs containing the heart, great vessels, trachea, etc.) appears within normal limits in terms of size and contour. * **Heart Size:** The heart size appears normal. * **Bones:** The ribs and clavicles appear intact. * **Diaphragm:** The diaphragms are seen. **Differential Diagnosis:** Based on the image, the differential diagnosis includes: * Lung cancer * Infection (pneumonia, abscess) * Pleural effusion * Hemothorax * Atelectasis * Other masses or lesions **Recommendations:** Given the significant abnormality in the right hemithorax, further evaluation is warranted. This may include: * **CT Scan of the Chest:** A CT scan would provide more detailed information about the nature and extent of the opacity, as well as the surrounding structures. * **Bronchoscopy:** A bronchoscopy may be performed to obtain tissue samples for biopsy if a mass is suspected. * **Thoracentesis:** If a pleural effusion is present, thoracentesis (needle aspiration of fluid from the pleural space) may be performed to analyze the fluid. * **PET Scan:** A PET scan can help differentiate between benign and</p>
<p>Radiologist: Right pneumothorax</p>		

(A) A 29-year-old man with chest discomfort. Radiograph and CT showed pneumomediastinum and subcutaneous emphysema. Radiologist and AIRead reports were appropriate, whereas MAIRA-2 included comparison statements and MedGemma inferred medical information. Green=true positive/true negative; red=false positive/false negative; yellow=hallucination.

(B) A 26-year-old man with chest pain and pneumothorax. Lingshu failed to report the large right pneumothorax, while other models described it correctly. MedVersa included a hallucinated statement regarding physician communication. Notably, MedGemma employed an enumerative manner, incorrectly characterizing the obvious compressive atelectasis caused by a large pneumothorax as mass/tumor, infection, fluid, or consolidation, thereby obscuring language clarity. Additionally, MedGemma's reports sometimes contained incomplete sentences. Green=true positive/true negative; red=false positive/false negative; yellow=hallucination/poor language clarity; underline=incomplete sentence.

Figure 6: Sensitivity and specificity for individual findings.



Forest plots show the sensitivity (left) and specificity (right) with 95% confidence intervals for 15 findings, including cardiomegaly, consolidation or ground-glass opacity (GGO), pleural effusion, pneumothorax, pneumomediastinum, hilar enlargement, mediastinal widening, reticular opacity, nodule or mass, emphysema, aortic aneurysm, cavity, pericardial effusion, miliary nodule, and pneumoperitoneum. Results are compared across five vision-language models (AIRead, Lingshu, MAIRA-2, MedGemma, and MedVersa) and radiologists (i.e., original reports).

Supplementary Texts

Supplementary Text 1: Medical image–specific vision–language models

1) AIRead: AIRead was designed to generate reports from frontal chest radiographs (CXRs) (either anteroposterior or posteroanterior view). The model comprises an image encoder and a language model; the encoder localizes potential abnormal regions and assigns 61 finding categories, and these outputs are passed to the language model for report generation. The model contains 2.6 billion parameters. The performance of an early version has been reported previously^{1,2}. The initial training dataset comprised approximately 14 million CXRs paired with reports, retrospectively collected from 11 tertiary hospitals in Korea and from multiple hospitals and clinics in the United States, of which 8 million image–report pairs were used to train the image encoder. Unlike the other models used in our experiments, the parameters of AIRead are not publicly available. However, the model can be accessed at <https://airead.soombit.ai/>, and the version used in this study was v0.2.5. This model is for research use only and has not been cleared or approved by regulatory authorities for clinical use.

2) Lingshu: Lingshu emphasizes comprehensive data curation to enhance medical artificial intelligence reasoning across multiple tasks, including multimodal question answering, text-based question answering, and medical report generation³. The model accepts diverse imaging modalities such as plain radiograph, CT, MRI, ultrasound, dermoscopy, fundus photography, histopathology, and microscopy. The training dataset comprised 2.55 million instances, with x-ray images accounting for 13%. Lingshu was built on the Qwen2.5-VL-Instruct model, with 7 billion and 32 billion parameters. In a pilot evaluation with a thoracic radiologist, the 32B model performed comparably to the 7B model for CXR report generation. Therefore, for these experiments, we used the 7B parameters available at <https://huggingface.co/lingshu-medical-mlm/Lingshu-7B>, and followed the inference recommendations provided in the model card.

3) MAIRA-2: MAIRA-2 was developed to provide comprehensive support for radiologists in interpreting CXRs by leveraging both frontal and lateral views, prior studies, and clinical indication⁴. The model further enhances report interpretation through a novel task termed grounded report

generation, which explicitly localizes each finding within the image. MAIRA-2 consists of an image encoder and a large language model with a visual adapter, using the radiology-specialized Rad-DINO-MAIRA-2 as the image encoder and Vicuna 7B v1.5 as the language model. The total model size is approximately 6.9 billion parameters. The training dataset included 510K image-report pairs from MIMIC-CXR, PadChest, USMix, and IU-Xray. For these experiments, we used the model parameters available at <https://huggingface.co/microsoft/maira-2>. For inference, we used “without grounding option”, since the quality of the report only differs slightly as described in the model card.

4) MedGemma: MedGemma is a medical foundation model designed to perform across diverse clinical tasks while reducing task-specific tuning requirements, thereby accelerating the development of artificial intelligence for healthcare applications⁵. Its vision module processes four imaging domains: radiology (CXRs, CT, MRI), histopathology, dermatology, and ophthalmology. Supported tasks include medical visual question answering, medical image classification, CXR report generation, and related applications. The architecture comprises a visual encoder and a language model connected via a visual adapter; the visual encoder is fine-tuned from SigLIP, and the language model is based on Gemma 3. Similar to MedVersa, MIMIC-CXR was the primary training dataset for CXR report generation. MedGemma is released in multiple variants, including instruction-tuned and pre-trained models, with parameter sizes ranging from 4 billion to 27 billion. At the start of this study, the 27B multimodal model was not available; therefore, we used the 4B instruction-tuned model (<https://huggingface.co/google/medgemma-4b-it>) and followed the inference recommendations provided in the model card.

5) MedVersa: MedVersa is a medical artificial intelligence generalist developed for diverse tasks in medical image interpretation⁶. It was trained on 13 million annotated instances spanning 11 tasks across 3 imaging modalities: CXRs, CT scans, and dermoscopic images. Supported tasks include report generation, open-ended visual question answering, and related applications. For CXR report generation, the primary training dataset was MIMIC-CXR. After filtering, MedVersa utilized approximately 122K CXRs paired with reports. The model consists of a 2D/3D visual encoder and a large language model,

with an adapter employed to transfer visual information to the language model. The total model size is approximately 6.9 billion parameters. For these experiments, we used the model parameters available at https://huggingface.co/hy Zhou/MedVersa_Internal. For CXR report generation, we followed the recommendations provided in the model card, including the specified environment setup.

6) Inference settings: All inferences were performed on a single NVIDIA H100 graphics processing unit with CUDA 12.4. To minimize the effects of stochastic variation in the generation process, greedy decoding was used to generate reports across all methods. Because the evaluation of this study focused on reports from a single frontal CXR, models capable of incorporating prior reports, additional images (including lateral views), or clinical information (e.g., age) were instead provided with blank or no inputs for these fields.

Supplementary Text 2: Details of a large language model–based labeler for extracting abnormal findings from free-text chest radiograph reports

A practical approach to quantitatively assess report-generation models is to compare labels extracted from model-generated and radiologist-written free-text reports. To this end, model-based labelers such as RadGraph and CheXpert++ have been developed to extract predefined labels and relations from radiology reports^{7,8}. More recently, leveraging the medical knowledge embedded in large language models (LLMs) has emerged as a promising direction for label extraction. In this line of work, CheXGPT utilized LLM-based medical knowledge to extract 13 labels (atelectasis, consolidation, effusion, fracture, hyperinflation, lung opacity, nodule, pleural lesion, pneumothorax, pulmonary edema, subcutaneous emphysema, subdiaphragmatic gas, widened mediastinal silhouette)⁹. CheXGPT also distilled the knowledge of a LLM into a lightweight language model, thereby enabling efficient label extraction and supporting a wide range of clinical applications.

For this study, we developed a labeler similar to CheXGPT by leveraging LLMs to extract labels, but the coverage extended from 13 to 76 abnormal categories. We adopted a similar training strategy, in which pseudo-label sets were first extracted from chest radiograph reports by using a LLM. These pseudo-labels were refined through domain-specific post-processing and subsequently used to supervise the training of a Bidirectional Encoder Representations from Transformers-based extraction model¹⁰.

References

1. Hong, E.K. et al. Diagnostic Accuracy and Clinical Value of a Domain-specific Multimodal Generative AI Model for Chest Radiograph Report Generation. *Radiology*. **314**, 241476; 10.1148/radiol.241476 (2025).
2. Hong, E.K. et al. Value of Using a Generative AI Model in Chest Radiography Reporting: A Reader Study. *Radiology*. **314**, 241646; 10.1148/radiol.241646 (2025).
3. Xu, W. et al. Lingshu: A Generalist Foundation Model for Unified Multimodal Medical Understanding and Reasoning. *arXiv:2506.07044* <https://arxiv.org/abs/2506.07044> (2025).
4. Bannur, S. et al. MAIRA-2: Grounded Radiology Report Generation. *arXiv:2406.04449* <https://arxiv.org/abs/2406.04449> (2024).
5. Sellergren, A. et al. MedGemma Technical Report. *arXiv:2507.05201* <https://arxiv.org/abs/2507.05201> (2025).
6. Zhou, H.Y. et al. MedVersa: A Generalist Foundation Model for Medical Image Interpretation. *arXiv:2405.07988* <https://arxiv.org/abs/2405.07988> (2024).
7. Jain, S. et al. RadGraph: Extracting Clinical Entities and Relations from Radiology Reports. *arXiv:2106.14463* <https://arxiv.org/abs/2106.14463> (2021).
8. McDermott, M.B.A., Hsu, T.M.H., Weng, W.H., Ghassemi, M. & Szolovits, P. CheXpert++: Approximating the CheXpert labeler for Speed, Differentiability, and Probabilistic Output. *arXiv:2006.15229* <https://arxiv.org/abs/2006.15229> (2020).
9. Gu, J. et al. CheX-GPT: Harnessing Large Language Models for Enhanced Chest X-ray Report Labeling. *arXiv:2401.11505* <https://arxiv.org/abs/2401.11505> (2024).
10. Devlin, J., Chang, M.W., Lee, K., Toutanova, K. BERT: Pre-training of Deep Bidirectional Transformers for Language Understanding. *arXiv:1810.04805* <https://arxiv.org/abs/1810.04805> (2018).

Supplementary Tables

Supplementary Table 1: Summarization of Evaluation Metrics

Criteria	Details
RADPEER score	
1	Agree with interpretations.
2	Disagree with interpretations which are understandable misses.
	a: unlikely to be clinically significant.
	b: likely to be clinically significant.
3	Disagree with interpretations which are unacceptable misses.
	a: unlikely to be clinically significant.
	b: likely to be clinically significant.
Clinical acceptability	
1: Not acceptable	The report contains major factual errors (e.g., missed referable findings, false-positive findings, incorrect laterality or diagnosis) that make it unsafe for clinical use. The content is misleading or unreliable and cannot be used even after editing.
2: Acceptable only with major revision	The report contains one or more significant problems (e.g., omission of a finding, vague or clinically misleading wording, or potentially harmful misinterpretation) that require extensive edits across multiple sentences or restructuring. A radiologist would need to spend meaningful time reviewing and rewriting the report before it could be used.
3: Acceptable only with minor revision	The report is generally accurate and includes key findings, but may have minor issues such as slightly awkward phrasing, limited detail (e.g., lacking severity), or subtle clarification needs. It can be used after quick edits without changing core content.
4: Acceptable as is	The report is accurate, clear, and clinically actionable as written. It requires no edits and could be signed and submitted directly.
Hallucination	The presence of information that could not be derived solely from a single frontal radiograph, in which

	information on scale was not available (e.g., references to a lateral view, clinical history, comparative statements, or size or distance descriptions).
Language clarity	Subjective scoring using a 5-point scale (1 = unacceptable, 2 = poor, 3 = moderate, 4 = good, 5 = excellent).

Supplementary Table 2: Subgroup Analysis in Men

Variable	Radiologist	AIRead	Lingshu	MAIRA-2	MedGemma	MedVersa
RADPEER Score 3b, %	13.4 (113/846)	5.6 (47/846)	42.9 (363/846)	24.2 (205/846)	17.1 (145/846)	24.7 (209/846)
P Value	Reference	<.001	<.001	<.001	.01	<.001
RADPEER Score 2b or 3b, %	27.8 (235/846)	18.8 (159/846)	55.6 (470/846)	34.5 (292/846)	27.5 (233/846)	35.2 (298/846)
P Value	Reference	<.001	<.001	<.001	.90	<.001
Clinically Acceptable Reports by Standard Criterion, %	76.4 (646/846)	85.2 (721/846)	42.3 (358/846)	67.5 (571/846)	71.7 (607/846)	67.1 (568/846)
P Value	Reference	<.001	<.001	<.001	.01	<.001
Clinically Acceptable Reports by Stringent Criterion, %	46.2 (391/846)	59.6 (504/846)	26.7 (226/846)	38.1 (322/846)	42.7 (361/846)	42.7 (361/846)
P Value	Reference	<.001	<.001	<.001	.07	.07
Hallucination, %	0.1 (1/846)	0.4 (3/846)	6.9 (58/846)	19.3 (163/846)	5.0 (42/846)	11.5 (97/846)
P Value	Reference	.33	<.001	<.001	<.001	<.001
Clarity of Language, %	76.6 (648/846)	82.9 (701/846)	89.2 (755/846)	77.9 (659/846)	69.4 (587/846)	87.9 (744/846)
P Value	Reference	.001	<.001	.52	.001	<.001

Clinical acceptability was defined as “acceptable as is” or “with minor revision” (standard), and strictly as “acceptable as is” only (stringent).

Clarity of language was defined as a score of 4 or higher (good to excellent).

P values represent comparisons against the radiologist as the reference.

Supplementary Table 3: Subgroup Analysis in Women

Variable	Radiologist	AIRead	Lingshu	MAIRA-2	MedGemma	MedVersa
RADPEER Score 3b, %	14.8 (87/588)	4.9 (29/588)	43.0 (253/588)	25.0 (147/588)	16.3 (96/588)	27.6 (162/588)
P Value	Reference	<.001	<.001	<.001	.41	<.001
RADPEER Score 2b or 3b, %	34.0 (200/588)	22.4 (132/588)	59.4 (349/588)	40.1 (236/588)	28.4 (167/588)	43.0 (253/588)
P Value	Reference	<.001	<.001	.01	.02	<.001
Clinically Acceptable Reports by Standard Criterion, %	71.3 (419/588)	83.5 (491/588)	39.3 (231/588)	62.9 (370/588)	70.9 (417/588)	58.8 (346/588)
P Value	Reference	<.001	<.001	<.001	.88	<.001
Clinically Acceptable Reports by Stringent Criterion, %	39.6 (233/588)	56.1 (330/588)	23.3 (137/588)	36.2 (213/588)	43.2 (254/588)	35.5 (209/588)
P Value	Reference	<.001	<.001	.15	.14	.08
Hallucination, %*	0 (0/579)	0.2 (1/579)	17.1 (99/579)	14.7 (85/579)	6.0 (35/579)	13.5 (78/579)
P Value	Reference	N/A	N/A	N/A	N/A	N/A
Clarity of Language, %	80.3 (472/588)	83.0 (488/588)	86.2 (507/588)	79.1 (465/588)	70.2 (413/588)	89.1 (524/588)
P Value	Reference	.22	.006	.61	<.001	<.001

Clinical acceptability was defined as “acceptable as is” or “with minor revision” (standard), and strictly as “acceptable as is” only (stringent).

Clarity of language was defined as a score of 4 or higher (good to excellent).

P values represent comparisons against the radiologist as the reference.

*Three patients whose original reports contained measurements were excluded from the analysis of hallucinations.

N/A = not available.

Supplementary Table 4: Subgroup Analysis of Patients Aged 65 Years and Older

Variable	Radiologist	AIRead	Lingshu	MAIRA-2	MedGemma	MedVersa
RADPEER Score 3b, %	17.7 (140/792)	5.7 (45/792)	47.5 (376/792)	30.7 (243/792)	19.2 (152/792)	29.9 (237/792)
P Value	Reference	<.001	<.001	<.001	.38	<.001
RADPEER Score 2b or 3b, %	37.4 (296/792)	21.8 (173/792)	63.5 (503/792)	42.4 (336/792)	29.9 (237/792)	43.2 (342/792)
P Value	Reference	<.001	<.001	.02	<.001	.008
Clinically Acceptable Reports by Standard Criterion, %	69.7 (552/792)	85.0 (673/792)	34.0 (269/792)	58.6 (464/792)	68.2 (540/792)	58.6 (464/792)
P Value	Reference	<.001	<.001	<.001	.45	<.001
Clinically Acceptable Reports by Stringent Criterion, %	29.8 (236/792)	50.6 (401/792)	14.8 (117/792)	26.3 (208/792)	33.7 (267/792)	29.9 (237/792)
P Value	Reference	<.001	<.001	.08	.06	.95
Hallucination, %*	0.1 (1/786)	0.5 (4/786)	12.5 (98/786)	21.0 (165/786)	7.6 (60/786)	12.8 (101/786)
P Value	Reference	.21	<.001	<.001	<.001	<.001
Clarity of Language, %	79.2 (627/792)	84.6 (670/792)	84.3 (668/792)	73.4 (581/792)	67.2 (532/792)	85.6 (678/792)
P Value	Reference	.004	.006	.005	<.001	.001

Clinical acceptability was defined as “acceptable as is” or “with minor revision” (standard), and strictly as “acceptable as is” only (stringent).

Clarity of language was defined as a score of 4 or higher (good to excellent).

P values represent comparisons against the radiologist as the reference.

*Two patients whose original reports contained measurements were excluded from the analysis of hallucinations.

Supplementary Table 5: Subgroup Analysis in Patients Younger Than 65 Years

Variable	Radiologist	AIRead	Lingshu	MAIRA-2	MedGemma	MedVersa
RADPEER Score 3b, %	9.3 (60/642)	4.8 (31/642)	37.4 (240/642)	17.0 (109/642)	13.9 (89/642)	20.9 (134/642)
P Value	Reference	<.001	<.001	<.001	.003	<.001
RADPEER Score 2b or 3b, %	21.7 (139/642)	18.4 (118/642)	49.2 (316/642)	29.9 (192/642)	25.4 (163/642)	32.6 (209/642)
P Value	Reference	.09	<.001	<.001	.06	<.001
Clinically Acceptable Reports by Standard Criterion, %	79.9 (513/642)	84.0 (539/642)	49.8 (320/642)	74.3 (477/642)	75.4 (484/642)	70.1 (450/642)
P Value	Reference	.03	<.001	.004	.02	<.001
Clinically Acceptable Reports by Stringent Criterion, %	60.4 (388/642)	67.4 (433/642)	38.3 (246/642)	50.9 (327/642)	54.2 (348/642)	51.9 (333/642)
P Value	Reference	.001	<.001	<.001	.004	<.001
Hallucination, %*	0 (0/639)	0 (0/639)	9.2 (59/639)	13.0 (83/639)	2.7 (17/639)	11.6 (74/639)
P Value	Reference	N/A	N/A	N/A	N/A	N/A
Clarity of Language, %	76.8 (493/642)	80.8 (519/642)	92.5 (594/642)	84.6 (543/642)	72.9 (468/642)	91.9 (590/642)
P Value	Reference	.07	<.001	<.001	.10	<.001

Clinical acceptability was defined as “acceptable as is” or “with minor revision” (standard), and strictly as “acceptable as is” only (stringent).

Clarity of language was defined as a score of 4 or higher (good to excellent).

P values represent comparisons against the radiologist as the reference.

*One patient whose original report included a measurement was excluded from the hallucination analysis.

N/A = not available.

Supplementary Table 6: Subgroup Analysis of Chest Radiograph Reports by Resident Radiologists

Variable	Radiologist	AIRead	Lingshu	MAIRA-2	MedGemma	MedVersa
RADPEER Score 3b, %	13.3 (143/1074)	5.6 (60/1074)	43.3 (465/1074)	24.0 (258/1074)	15.4 (165/1074)	25.3 (272/1074)
P Value	Reference	<.001	<.001	<.001	.12	<.001
RADPEER Score 2b or 3b, %	29.3 (315/1074)	20.9 (225/1074)	56.5 (607/1074)	36.1 (388/1074)	26.6 (286/1074)	37.7 (405/1074)
P Value	Reference	<.001	<.001	<.001	.11	<.001
Clinically Acceptable Reports by Standard Criterion, %	75.1 (807/1074)	84.4 (906/1074)	41.4 (445/1074)	65.9 (708/1074)	72.9 (783/1074)	64.5 (693/1074)
P Value	Reference	<.001	<.001	<.001	.16	<.001
Clinically Acceptable Reports by Stringent Criterion, %	45.3 (487/1074)	58.3 (626/1074)	26.0 (279/1074)	37.2 (400/1074)	44.8 (481/1074)	40.5 (435/1074)
P Value	Reference	<.001	<.001	<.001	.75	.005
Hallucination, %*	0.1 (1/1065)	0.3 (3/1065)	11.2 (119/1065)	16.8 (179/1065)	3.9 (42/1065)	12.1 (129/1065)
P Value	Reference	.34	<.001	<.001	<.001	<.001
Clarity of Language, %	77.8 (836/1074)	83.1 (892/1074)	88.5 (951/1074)	79.2 (851/1074)	69.8 (750/1074)	88.5 (951/1074)
P Value	Reference	.002	<.001	.42	<.001	<.001

Clinical acceptability was defined as “acceptable as is” or “with minor revision” (standard), and strictly as “acceptable as is” only (stringent).

Clarity of language was defined as a score of 4 or higher (good to excellent).

P values represent comparisons against the radiologist as the reference.

*Three patients whose original reports included a measurement were excluded from the hallucination analysis.

Supplementary Table 7: Subgroup Analysis of Chest Radiograph Reports by Board-Certified Radiologists

Variable	Radiologist	AIRead	Lingshu	MAIRA-2	MedGemma	MedVersa
RADPEER Score 3b, %	15.8 (57/360)	4.4 (16/360)	41.9 (151/360)	26.1 (94/360)	21.1 (76/360)	27.5 (99/360)
P Value	Reference	<.001	<.001	<.001	.04	<.001
RADPEER Score 2b or 3b, %	33.3 (120/360)	18.3 (66/360)	58.9 (212/360)	38.9 (140/360)	31.7 (114/360)	40.6 (146/360)
P Value	Reference	<.001	<.001	.07	.58	.02
Clinically Acceptable Reports by Standard Criterion, %	71.7 (258/360)	85.0 (306/360)	40.0 (144/360)	64.7 (233/360)	66.9 (241/360)	61.4 (221/360)
P Value	Reference	<.001	<.001	.02	.11	.001
Clinically Acceptable Reports by Stringent Criterion, %	38.1 (137/360)	57.8 (208/360)	23.3 (84/360)	37.5 (135/360)	37.2 (134/360)	37.5 (135/360)
P Value	Reference	<.001	<.001	.85	.78	.85
Hallucination, %	0 (0/360)	0.3 (1/360)	10.6 (38/360)	19.2 (69/360)	9.7 (35/360)	12.8 (46/360)
P Value	Reference	N/A	N/A	N/A	N/A	N/A
Clarity of Language, %	78.9 (284/360)	82.5 (297/360)	86.4 (311/360)	75.8 (273/360)	69.4 (250/360)	88.1 (317/360)
P Value	Reference	.21	.007	.32	.003	.001

Clinical acceptability was defined as “acceptable as is” or “with minor revision” (standard), and strictly as “acceptable as is” only (stringent).

Clarity of language was defined as a score of 4 or higher (good to excellent).

P values represent comparisons against the radiologist as the reference.

N/A = not available.